Journal of Power Sources 196 (2011) 4724–4728

Contents lists available at ScienceDirect

Journal of Power Sources

journal homepage: www.elsevier.com/locate/jpowsour

Short communication

Catalytic activity of bimetallic nickel alloys for solid-oxide fuel cell anode reactions from density-functional theory

Wei An[a], Daniel Gatewood[b], Brett Dunlap[b], C. Heath Turner[a,*]

[a] Department of Chemical and Biological Engineering, The University of Alabama, Box 870203, Tuscaloosa, AL 35487-0203, United States
[b] Chemistry Division, Code 6189, Naval Research Laboratory, Washington, DC 20375, United States

ARTICLE INFO

Article history:
Received 22 October 2010
Received in revised form
22 December 2010
Accepted 4 January 2011
Available online 14 January 2011

Keywords:
SOFC
DFT
Adsorption
Anode
Nickel
Alloy

ABSTRACT

We present density-functional theory calculations of the chemisorption of atomic species O, S, C, H and reaction intermediates OH, SH, and CH_n (n = 1, 2, and 3) on M/Ni alloy model catalysts (M = Bi, Mo, Fe, Co, and Cu). The activity of the Ni alloy catalysts for solid-oxide fuel cell (SOFC) anode oxidation reactions is predicted, based on a simple descriptor, i.e., the binding energy of oxygen. First, we find that the binding of undesirable intermediates, such as C and S, can be inhibited and the catalytic activity of planar Ni-based anodes can be tuned towards oxidation by selectively forming a bimetallic surface alloy. In particular, Cu/Ni, Fe/Ni, and Co/Ni anode catalysts are found to be most active towards anode oxidation. On the other hand, the Mo/Ni alloy surface is predicted to be the most effective catalyst in terms of inhibiting the deposition of C and S (while still preserving relatively high catalytic activity). The formation of a surface alloy, which has the alloy element enriched on the topmost surface, was found to be critical to the activity of the Ni alloy catalysts.

1. Introduction

Solid-oxide fuel cells (SOFCs) have emerged as a promising technology for efficient electrochemical energy conversion. In addition, their fuel flexibility enables the direct utilization of natural gas by internal steam reforming [1,2]. A typical SOFC contains four basic components: anode, electrolyte, cathode, and interconnect. For many years, yttria-stabilized zirconia (YSZ) has been commonly used as the electrolyte, and a Ni/YSZ cermet has served as the anode, which is where the fuel is electrocatalytically oxidized at the three-phase boundary (TPB) of the fuel/electrode/electrolyte. SOFCs typically operate at high temperatures (in the range of 800–1000 °C), which enables high ionic conductivity (O^{2-} diffusivity) within the YSZ lattice, superior catalytic activity of the Ni-based anode towards oxidation of the fuel (mainly H_2 and CO), and steam reforming of hydrocarbons. However, the high operating temperatures also cause severe materials degradation, application limitations, and high integration costs.

The catalytic performance of the anode in a SOFC plays a key role in determining the overall fuel cell performance. The development of optimal anode materials (i.e., combinations of electrode and electrolyte) with high catalytic activity at lower temperatures (i.e., 500–800 °C) has been an active research topic [3–11]. Although a number of material candidates have been considered (see latest review [12] and references therein), Ni-cermet-based materials still remain the most efficient and practical anode materials. This is in large part due to the fact that the basic properties of such 'standard' Ni-zirconia or Ni-ceria cermets are well-established. In particular, they possess superior catalytic activity, electrical conductivity, and gaseous diffusivity, as well as excellent structural integrity under operating conditions. Hence, further development of Ni-cermet-based anodes should be realized by fabricating optimal microstructures and by identifying moderate compositional optimization of existing Ni-cermet systems [3–9]. By pursuing this route, the inherent catalytic functionality and compatibility with the other components in the fuel cell and the fuel cell stack should be conserved.

One of the main advantages of Ni-cermet-based anodes is the high electrocatalytic activity of Ni towards H_2, CO, hydrocarbon oxidation, and catalytic activity of Ni towards steam reforming of methane (SRM) under operating conditions. However, Ni also catalyzes the formation of carbon from hydrocarbons under reducing conditions [13], which can block active Ni sites. In addition, the Ni catalyst is easily poisoned by sulfur (a common impurity in natural gas), which can also block active Ni sites and possibly diffuse inside nickel. In certain cases, Ni–S eutectic liquids can even be formed under operating conditions [14]. Ultimately, carbon deposition and sulfur poisoning will lead to the deactivation of the anode

* Corresponding author. Tel.: +1 205 348 1733; fax: +1 205 348 7558.
E-mail address: hturner@eng.ua.edu (C.H. Turner).

0378-7753/$ – see front matter © 2011 Elsevier B.V. All rights reserved.
doi:10.1016/j.jpowsour.2011.01.007

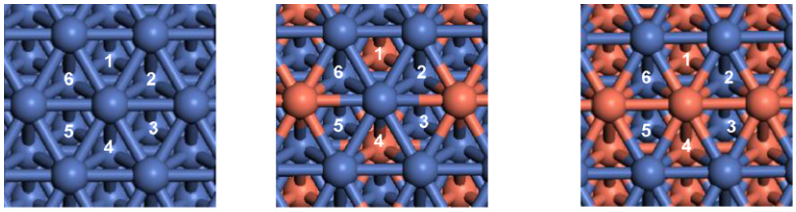

Fig. 1. Optimized (1 1 1) surfaces with various 3-fold hollow sites labeled: (a) Ni, (b) $Ni_{0.75}Cu_{0.25}$, and (c) $Ni_{0.5}Cu_{0.5}$. Blue = Ni and orange = Cu. (For interpretation of the references to color in this figure legend, the reader is referred to the web version of the article.)

and loss of its durability. Therefore, further development requires Ni-based anodes with enhanced tolerance to coking and sulfur poisoning. With respect to the selection of alternate anode materials, many other transition metals besides Ni have been investigated; however, none of them are able to compete with and replace Ni completely, in terms of performance and cost [12,15,16]. On the other hand, Ni-alloys can help mitigate carbon- and sulfur-induced deactivation, while maintaining the inherent material structure and performance of the SOFC [17–22]. For instance, carbon formation can be suppressed by employing Ni surface alloys, such as Cu/Ni(1 1 1) [22,23] or Au/Ni(1 1 1) [24]. Furthermore, several experimental studies of Ni-alloy anodes have demonstrated the beneficial effects of the alloying element (e.g., Mo, Fe, Cu, Pd, and Sn) on the fuel cell performance [13,17–21].

In order to provide additional insights into the development of Ni-alloy anode materials, we employed density functional theory (DFT) to study the effects of different alloying elements on the catalytic properties. Mainly, we predict the binding energies of various adsorbates and reaction intermediates of SOFC anode reactions on bimetallic M/Ni(1 1 1) surface alloys (M = Bi, Mo, Fe, Co, and Cu). We calculate the adsorption of atomic species O, S, C, and H and reaction intermediates OH, SH, and CH_n (n = 1, 2, and 3) on Ni surface alloys, with different alloying compositions, and this information is used to quantify the expected catalytic activity for oxidation at the anode. We find that the binding of undesirable intermediates (C and S) can be suppressed, and the catalytic activity of the Ni-alloy anodes can be tuned towards oxidation by forming selective bimetallic M/Ni(1 1 1) surface alloys.

2. Methods

All calculations were performed using DFT, as implemented in the Vienna ab initio simulation package (VASP) [25]. The program uses a plane-wave basis set, thus offering good access to the Hellmann–Feynman forces acting on all of the atoms in the supercell. The spin-polarized GGA PBE functional [26], an all-electron plane-wave basis set with an energy cutoff of 400 eV, and the projector augmented wave (PAW) method [27,28] were adopted. The Brillouin-zone of the $p(2 \times 2)$ lateral supercell was sampled by $5 \times 5 \times 1$ k-points using the Monkhorst–Pack scheme, and first-order Methfessel–Paxton smearing [29] of 0.2 eV was employed in the integration to speed up the convergence. The optimization was performed using conjugate-gradient algorithm without symmetry constraints, and the convergence threshold was set to be 10^{-4} eV for total energy and 10^{-2} eV Å^{-1} in force on each atom. All of the reported energies were extrapolated to k_BT = 0 eV.

The Ni(1 1 1) surface was modeled by a four-layer slab, with the lower two layers fixed at their equilibrium bulk phase positions (calculated lattice constant = 3.522 Å), while the upper two layers were allowed to relax. The two successive slabs were separated by a 13 Å vacuum region to ensure that the adsorbates (i.e., O, S, C, H, OH, SH, and CH_n, n = 1, 2 and 3) and the subsequent slab would not interact. The M/Ni(1 1 1) surface alloy (M = Bi, Mo, Fe, Co, and Cu) was modeled in the same fashion as the pure Ni(1 1 1) surface. However, in the alloy, the Ni atoms were substituted with M atoms on the topmost layer in the optimized $p(2 \times 2)$ lateral supercell, with four metal atoms in each of the four layers of the slab supercell, as shown in Fig. 1. The M/Ni(1 1 1) surface alloys were constructed, with θ = 1/4 and 1/2 ML (in terms of M coverage) by substituting one or two of the surface nickel atoms with M atoms. Alternatively for copper, Cu/Ni(1 1 1) surfaces were also cleaved from a NiCu bulk alloy having one, Fig. 1(b), or two, Fig. 1(c), copper atoms in each layer.

The binding energy (BE) in this work is defined as $BE = E_{total}[slab] + E_{total}[adsorbate] - E_{total}[slab + adsorbate]$, where E_{total} is the total energy of the system in one supercell, and the gas-phase adsorbate is used as the reference for E_{total}[adsorbate].

3. Results and discussion

In general, the net SOFC electrode reactions can be written as (all molecules are in the gas phase and all atomic and intermediate species are in adsorbed states):

$$\text{Anode}: \quad H_2 + O^{2-}(\text{electrolyte}) \rightarrow H_2O + 2e^- \tag{1}$$

$$CO + O^{2-}(\text{electrolyte}) \rightarrow CO_2 + 2e^- \tag{2}$$

$$\text{Cathode}: \quad O_2 + 4e^- \rightarrow 2O^{2-}(\text{electrolyte}) \tag{3}$$

$$\text{Overall reaction}: \quad CO + H_2 + O_2 \rightarrow CO_2 + H_2O \tag{4}$$

If natural gas is used as the fuel, the internal steam reforming of hydrocarbons (mainly methane) also occurs at the anode:

$$CH_4 + H_2O \rightarrow CO + 3H_2 \tag{5}$$

The overall reactions in (4) and (5) consist of a number of elementary reactions involving atomic species such as O, S (as an impurity in natural gas), C, and H, and reaction intermediates such as OH, SH, and CH_n (n = 1, 2 and 3). Therefore, the binding nature of these atomic species is relevant to the catalytic performance and deactivation of the SOFC anode. According to the "Sabatier principle", a good catalyst has active sites which bind reaction intermediates with an intermediate strength. In other words, binding that is too weak or too strong leads to a catalyst which is either less active or easily poisoned. In particular, the chemical interaction between the atomic O and the anode is believed to play a critical role in the overall fuel cell performance [15,16]. It should be noted that the fundamental mechanisms associated with the electrochemistry

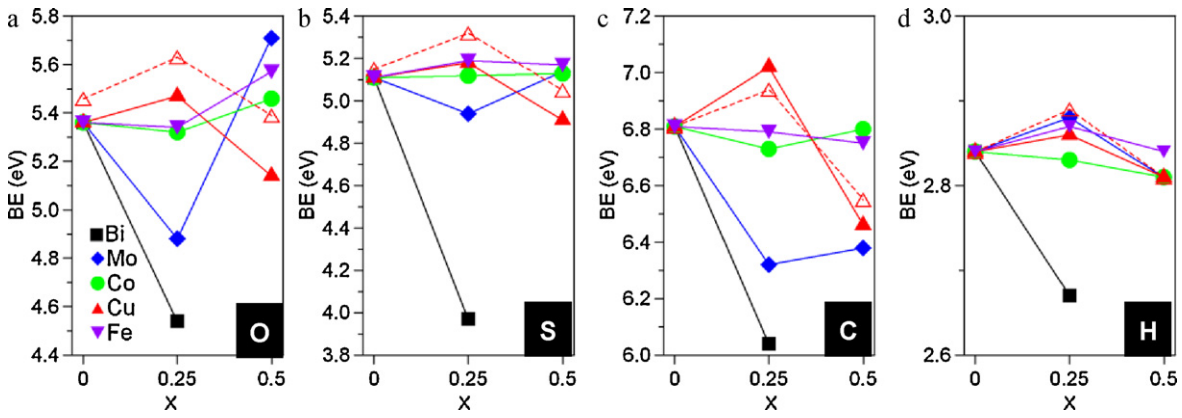

Fig. 2. Maximum binding energy (BE) of atomic species on $Ni_{(1-x)}M_x$ (1 1 1) surface alloys, as a function of mole fraction (x): (a) O, (b) S, (c) C and (d) H. Black, blue, purple, green, and red, denote M = Bi (■), Mo (◆), Fe (▼), Co (●), and Cu (▲ and △), respectively. Hollow red triangles represent the surface cleaved from a stoichiometric $Ni_{(1-x)}Cu_x$ bulk alloy. (For interpretation of the references to color in this figure legend, the reader is referred to the web version of the article.)

in reaction (4) are still not completely understood [30]. Two main reaction mechanisms at the anode have been widely proposed: (i) oxygen spillover; (ii) hydrogen spillover. In the former pathway, O^{2-} migrates from the YSZ electrolyte to the Ni surface forming adsorbed O species, which oxidize the fuel (i.e., CO and H_2):

$$O^{2-}(\text{electrolyte}) \rightarrow O + 2e^- \quad (6)$$

In the latter pathway, H_2 diffuses through the porous Ni-cermet forming dissociated H atoms on the Ni surface, which subsequently release their electrons to the Ni electrode and hop to the O^{2-} or OH^- site on the ceramic, YSZ, forming water. The neutralization (charge interactions) of the acidic H^+ and the basic O^{2-} or OH^- on YSZ serves as the driving force for proton migration. In both pathways, the electrons (without passing through the ion conductive electrolyte) are directed towards the cathode through an external circuit, which creates electrical current. The "oxygen spillover" mechanism also explains the electrochemical oxidation of CO without the involvement of H_2. Thus, we use the binding of atomic O on the metal as a key descriptor for the performance of the proposed M/Ni alloy catalysts.

3.1. Adsorption of atomic species

For the anode oxidation to proceed, the fuel, i.e., hydrogen and hydrocarbons, must be chemisorbed and dissociated into atomic species, which must further react with adsorbed O at the TPB. We first investigated the adsorption of atomic species O, S, C, and H on various M/Ni(1 1 1) alloys (M = Bi, Mo, Fe, Co, and Cu). We began these calculations by first investigating the influence of the surface composition on the adsorption, versus the influence of the bulk catalyst composition.

Fig. 2 shows the maximum binding energy (BE) of these atomic species as a function of the mole fraction (x) of M on the $Ni_{(1-x)}M_x$(1 1 1) alloy surfaces. We find that the most stable adsorption sites are: (1) the [Ni–Ni–Ni] 3-fold hollow sites on pure Ni(1 1 1) and on the M/Ni(1 1 1) alloy surfaces, with 0.25 ML coverage of M; and (2) the [Ni–Ni–M] 3-fold hollow sites on the M/Ni(1 1 1) alloy surface with 0.5 ML coverage of M (see Fig. 1). From Fig. 2, one can see that the incorporation of Bi has the most significant effect on reducing the binding strength of the O, S, C, and H atomic adsorbates. However, according to our calculated results, Bi is too large [31] and segregates above the surface if two Ni and two Bi atoms are in the surface layer. This only allows a maximum Bi coverage of 0.25 ML on a Bi/Ni(1 1 1) surface, in our modeling scheme, where each surface Ni atom has four surface Ni atoms and two surface Bi atoms as neighbors. In comparison, Mo, Fe, Co, and Cu (being smaller) can all form stable surface alloys at higher concentrations. At the higher 0.5 ML coverage of M, each Ni atom has two Ni atoms and four M atoms as neighbors, and equivalently each M atom has four Ni atoms and two M atoms as neighbors.

Comparatively, the Mo/Ni(1 1 1) surface alloy with 0.25 ML coverage of Mo has the best performance in terms of lowering the binding strength of C and S, while maintaining the binding strength of O at a favorable level, which ensures a high catalytic activity towards oxidation (see Section 3.3). Our calculated results agree very well with the early experimental finding that doping the Ni anode with small quantities of molybdenum (<1%) leads to a significant reduction in carbon deposits, while having little effect on the SRM and SOFC performance [13]. If the Mo coverage is further increased up to 0.5 ML, there is a significant increase in the binding strength of O and a slight increase in the binding strength of S. Both values are higher than on a pure Ni(1 1 1) surface. The beneficial effect of Mo on inhibiting C adsorption remains intact, regardless of the higher Mo surface coverage. By contrast, the binding strength of H increases on the Ni alloy with 0.25 ML Mo, but the binding weakens at a coverage of 0.5 ML of Mo, as compared to that on a pure Ni(1 1 1) surface. Since the "hydrogen spillover" mechanism directly depends on the chemisorption of H atoms, which are further split into protons and electrons, this alternative reaction pathway can be sensitive to the binding of H atoms on Ni the alloy.

Likewise, the Fe/Ni and Co/Ni alloys demonstrate behavior similar to the Mo/Ni alloy, in terms of modifying the binding energy, but with a more moderate influence. The trend predicted from the Cu/Ni alloy surface is different from that of Bi, Mo, Fe, and Co. From Fig. 2, one can see that the binding strengths of O, S, C, and H are all enhanced at 0.25 ML of Cu and then weaken at 0.5 ML of Cu, as compared to those on a pure Ni(1 1 1) surface. This suggests that the beneficial effect of Cu on inhibiting S and C is more pronounced at higher Cu coverage, which agrees well with the experimental observations that Cu/Ni catalysts, with Cu concentrations up to 50%, have demonstrated the highest ratio of reforming:coking rates [32,33]. Our previous study also showed that Cu addition can inhibit carbon formation during the sequential dissociation of CH_4, as the activation energy barrier of the final step is increased [23].

As a comparison, we also investigated the adsorption behavior of O, S, C, and H on Cu/Ni(1 1 1) alloy surfaces [see Fig. 1(a) and (b)], cleaved from a Cu/Ni bulk alloy yielding the dashed lines in Fig. 2. One can see that the binding strength trends of the atomic species O, S, C, and H on the bulk Cu/Ni(1 1 1) alloy surface are very similar to the values calculated on the Cu/Ni(1 1 1) surface alloy (i.e., the model with the alloy element only present in the top layer). This

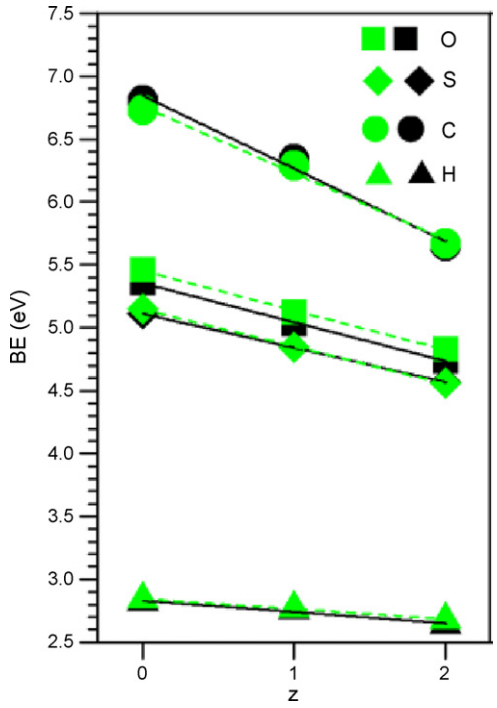

Fig. 3. Binding energy (BE) of fragments on (1 1 1) surfaces as a function of the number (z) of Cu atoms at *hcp* (black) and *fcc* (green) 3-fold hollow sites, as shown in Fig. 2, where z = 0, 1, 2 corresponds to (1 1 1) surfaces of Ni, $Ni_{0.75}Cu_{0.25}$, $Ni_{0.5}Cu_{0.5}$ bulk alloy, respectively. (For interpretation of the references to color in this figure legend, the reader is referred to the web version of the article.)

suggests that the alloy atoms in the topmost layer play the largest role in mediating the adsorbate binding strength, and thus the catalytic properties of the surface. Therefore, it is critical to know the precise surface alloy composition in the experimental systems. Furthermore, this provides supporting evidence that precious metal loading can be minimized, if the surface alloy composition can be maintained at the desired level.

As shown in Fig. 3, the BEs of O, S, C, and H decrease almost linearly as the number (z) of Cu atoms around the 3-fold hollow sites increases. This trend continues, regardless of the particular *hcp* or *fcc* site configuration, where z = 0, 1, and 2 corresponds to Ni, $Ni_{0.75}Cu_{0.25}$, and $Ni_{0.5}Cu_{0.5}$(1 1 1) surfaces, respectively. This illustrates the important effect of the alloying element in the ensemble of nearest-neighbor atoms. The deposition of C and S generally requires large Ni ensembles. By contrast, the adsorption of O, S, C, and H is enhanced at the [Ni–Ni–Ni] 3-fold hollow sites by Cu alloying (see Fig. 2), as a result of the Cu ligand effect.

3.2. Adsorption of reaction intermediates

In a high temperature SOFC, internal steam reforming of methane occurs either when wet natural gas is imported as a feedstock or as a result of the reaction of CH_4 with the H_2O produced from H_2 oxidation at the anode. It has been suggested that 'oxygen spillover' is the dominant reaction mechanism at the anode [16]. In this process, oxygen ions are transferred by surface spillover from the YSZ electrolyte to the Ni surface, followed by reaction with H and CH_n (produced from the dehydrogenation of CH_4). Adsorbed atomic O species, which can also be produced from the dissociation of H_2O on the Ni surface, play a key role in the SOFC anode reactions. At high operating temperatures (typical of SOFCs), CH_4 is most likely to be completely dehydrogenated to C, unless a much higher activation energy barrier exists to inhibit the final dehydrogenation step: CH → C + H. An alternate (and preferred) route is the oxidation of the CH species: CH + O → H + CO [31].

As shown in Fig. 4, we predict the adsorption of other reaction intermediates on the M/Ni(1 1 1) alloy surfaces, including: CH_n (n = 1, 2 and 3), OH, and SH fragments. The predictions are based on the calculated binding energy of A and using a scaling relationship to extrapolate the BEs of AH_n (A = C, O and S). This approach is described in more detail in Ref. [32], and it is expected to be applicable to Ni-based surface alloys [23]. From Fig. 4, one can see that when OH and SH are adsorbed at the same sites on the Ni(1 1 1) surface, the predicted BEs are quite close in energy. The same behavior is seen on the M/Ni(1 1 1) alloy surfaces, suggesting that OH and SH are competitive reaction intermediates during the elementary reaction processes. The BEs of CH_n, OH_n, and SH_n increase as n decreases (for C, O and S compare with Fig. 2), and this trend is consistent with the increase in the free bonding capability of the AH_n species. This increasing BE also serves as the driving force for the dissociation of CH_4, H_2O, and H_2S in the fuel, leading to the formation of the atomic species (i.e., C, O, and S) on the catalyst surface.

3.3. Catalytic activity of bimetallic M/Ni surface alloys for SOFC anode reactions

Previous studies have shown that oxygen spillover, where adsorbed O is a key intermediate, can be a dominant reaction channel under typical SOFC operating conditions [15,16]. This suggests that the BE of O may be used as a simple descriptor of the catalytic activity of the anode. In Fig. 5, we draw the characteristic volcano-type [33] plot of the calculated catalytic activity for a collection of anode oxidation reactions versus the O binding strength on (1 1 1) transition metal surfaces, with lines re-plotted from the study by Rossmeisl and Bessler [16]. In their study, Ni was identified as the best catalyst for the SOFC anode reactions among a number of transition metals, including Ru, Rh, Pd, Pt, and Au. It can be clearly seen that the bimetallic Ni-alloy systems studied in this

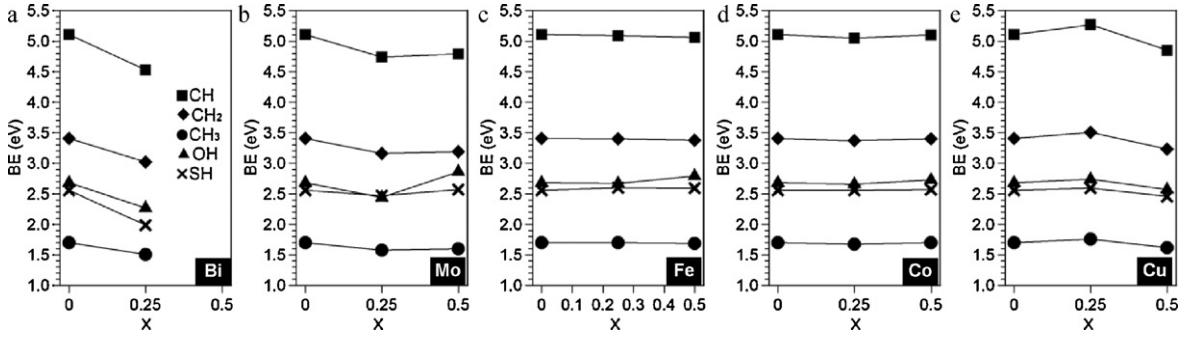

Fig. 4. Maximum binding energy (BE) of CH_n (n = 1, 2 and 3), OH, and SH fragments on $Ni_{(1-x)}M_x$ (1 1 1) surface alloys, as a function of the mole fraction (x): (a) Bi, (b) Mo, (c) Fe, (d) Co, and (e) Cu.

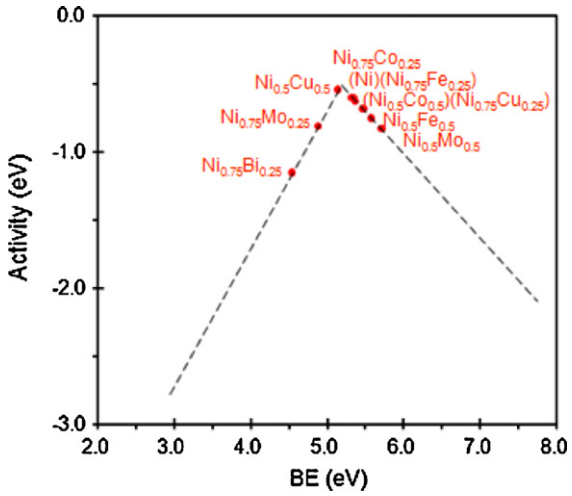

Fig. 5. The volcano curve of theoretical activity versus binding energy (BE) of O on (1 1 1) transition metal surfaces, re-plotted from Fig. 6 of Ref. [15].

work possess optimal activity, close to that of pure Ni. In particular, $Ni_{0.5}Cu_{0.5}$, $Ni_{0.75}Co_{0.25}$, $Ni_{0.75}Fe_{0.25}$, $Ni_{0.5}Co_{0.5}$, and $Ni_{0.75}Cu_{0.25}$ surface alloys have superior catalytic activity towards anode oxidation. Thus, improvements can be made, without abandoning the advantages of Ni (low cost, material compatibility, etc.). For example, our predications on NiFe surface alloys agree well with a very recent study [34], which shows that a NiFe bimetallic alloy used as an anode can significantly improve the maximum power density and lower the anodic overpotential at intermediate temperatures. Moreover, the addition of a small amount of Fe to Ni can drastically decrease the aggregation of Ni under the cell operating conditions.

4. Conclusions

The ideal materials choice for SOFC anodes is determined by a number of factors, such as catalytic activity, electrical conductivity, thermal compatibility, and chemical stability. Thus, the formation of Ni-alloy surfaces may provide advantages that improve the performance of existing Ni-cermet based anode materials. These efforts may lead to higher efficiency and a longer lifetime at lower operational temperatures. In this work, we report a DFT-based computational study on the effects of alloying elements on the adsorption of reaction intermediates, which are critical for quantifying the catalytic activity of bimetallic M/Ni(1 1 1) surface alloys (M = Bi, Mo, Fe, Co, and Cu) for SOFC anode reactions. We find that the binding of undesirable intermediates (i.e., C and S) can be suppressed and the catalytic activity of Ni-based anodes can be tuned towards oxidation by selectively forming bimetallic M/Ni(1 1 1) surface alloys. The Cu/Ni, Fe/Ni and Co/Ni systems appear to be most active towards anode oxidation, based on the correlation between the catalytic activity and the binding energy of O. On the other hand, the Mo/Ni alloy is the most effective catalyst, in terms of inhibiting the deposition of C and S, while still maintaining a high catalytic activity. The formation of a *surface* alloy is found to be critical to tuning the activity, and this is particularly important if precious metals are used as alloying elements, due to cost.

Acknowledgments

The Office of Naval Research directly and through the Naval Research Laboratory supported this research. Supercomputer resources were provided by the Alabama Supercomputer Center and the NCSA TeraGrid. A portion of the research was performed using EMSL, a national scientific user facility sponsored by the Department of Energy's Office of Biological and Environmental Research and located at Pacific Northwest National Laboratory.

References

[1] S.C. Singhal, Solid State Ionics 135 (2000) 305–313.
[2] A.B. Stambouli, E. Traversa, Renew. Sust. Energy Rev. 6 (2002) 433–455.
[3] T. Hibino, A. Hashimoto, T. Inoue, J. Tokuno, S. Yoshida, M. Sano, Science 288 (2000) 2031–2033.
[4] E.P. Murray, T. Tsai, S.A. Barnett, Nature 400 (1999) 649–651.
[5] S. de Souza, S.J. Visco, L.C. De Jonghe, Solid State Ionics 98 (1997) 57–61.
[6] T. Suzuki, Z. Hasan, Y. Funahashi, T. Yamaguchi, Y. Fujishiro, M. Awano, Science 325 (2009) 852–855.
[7] A. Ignatiev, X. Chen, N.J. Wu, Z.G. Lu, L. Smith, Dalton Trans. (2008) 5501–5506.
[8] S. Kang, P.C. Su, Y.I. Park, Y. Saito, F.B. Prinz, J. Electrochem. Soc. 153 (2006) A554–A559.
[9] C.J. Zhang, J. Grandner, R. Liu, S.B. Lee, B.W. Eichhorn, Phys. Chem. Chem. Phys. 12 (2010) 4295–4300.
[10] S.W. Tao, J.T.S. Irvine, Nat. Mater. 2 (2003) 320–323.
[11] H. Huang, M. Nakamura, P.C. Su, R. Fasching, Y. Saito, F.B. Prinz, J. Electrochem. Soc. 154 (2007) B20–B24.
[12] A.J. Jacobson, Chem. Mater. 22 (2010) 660–674.
[13] C.M. Finnerty, N.J. Coe, R.H. Cunningham, R.M. Ormerod, Catal. Today 46 (1998) 137–145.
[14] H. Kishimoto, T. Horita, K. Yamaji, M.E. Brito, Y.P. Xiong, H. Yokokawa, J. Electrochem. Soc. 157 (2010) B802–B813.
[15] T. Setoguchi, K. Okamoto, K. Eguchi, H. Arai, J. Electrochem. Soc. 139 (1992) 2875–2880.
[16] J. Rossmeisl, W.G. Bessler, Solid State Ionics 178 (2008) 1694–1700.
[17] T. Ishihara, J.W. Yan, M. Shinagawa, H. Matsumoto, Electrochim. Acta 52 (2006) 1645–1650.
[18] R.J. Gorte, S. Park, J.M. Vohs, C.H. Wang, Adv. Mater. 12 (2000) 1465–1469.
[19] H. Kim, C. Lu, W.L. Worrell, J.M. Vohs, R.J. Gorte, J. Electrochem. Soc. 149 (2002) A247–A250.
[20] H. Kan, S.H. Hyun, Y.G. Shul, H. Lee, Catal. Commun. 11 (2009) 180–183.
[21] Y. Nabae, I. Yamanaka, M. Hatano, K. Otsuka, J. Phys. Chem. C 112 (2008) 10308–10315.
[22] N.M. Galea, D. Knapp, T. Ziegler, J. Catal. 247 (2007) 20–33.
[23] W. An, X.C. Zeng, C.H. Turner, J. Chem. Phys. 131 (2009) 174702.
[24] F. Besenbacher, I. Chorkendorff, B.S. Clausen, B. Hammer, A.M. Molenbroek, J.K. Norskøv, I. Stensgaard, Science 279 (1998) 1913–1915.
[25] G. Kresse, J. Hafner, Phys. Rev. B 47 (1993) 558–561.
[26] J.P. Perdew, K. Burke, M. Ernzerhof, Phys. Rev. Lett. 77 (1996) 3865–3868.
[27] P.E. Blöchl, Phys. Rev. B 50 (1994) 17953–17979.
[28] G. Kresse, D. Joubert, Phys. Rev. B 59 (1999) 1758–1775.
[29] M. Methfessel, A.T. Paxton, Phys. Rev. B 40 (1989) 3616–3621.
[30] W.G. Bessler, M. Vogler, H. Stormer, D. Gerthsen, A. Utz, A. Weber, E. Ivers-Tiffee, Phys. Chem. Chem. Phys. 12 (2010) 13888–13903.
[31] D.W. Blaylock, T. Ogura, W.H. Green, G.J.O. Beran, J. Phys. Chem. C 113 (2009) 4898–4908.
[32] F. Abild-Pedersen, J. Greeley, F. Studt, J. Rossmeisl, T.R. Munter, P.G. Moses, E. Skulason, T. Bligaard, J.K. Norskøv, Phys. Rev. Lett. 99 (2007) 016105.
[33] J.K. Norskøv, J. Rossmeisl, A. Logadottir, L. Lindqvist, J.R. Kitchin, T. Bligaard, H. Jonsson, J. Phys. Chem. B 108 (2004) 17886–17892.
[34] T. Ishihara, H. Zhong, Scr. Mater. (2010) 022, doi:10.1016/j.scriptamat.2010.08.